Identification of Destabilized Metal Hydrides for Hydrogen Storage Using First Principles Calculations

Sudhakar V. Alapati,[†] J. Karl Johnson,[‡,§] and David S. Sholl*[,†,§]

Department of Chemical Engineering, Carnegie Mellon University, Pittsburgh, Pennsylvania 15213, Department of Chemical Engineering, University of Pittsburgh, Pittsburgh, Pennsylvania 15261, and National Energy Technology Laboratory, Pittsburgh, Pennsylvania 15236

Received: January 23, 2006; In Final Form: March 8, 2006

Hydrides of period 2 and 3 elements are promising candidates for hydrogen storage but typically have heats of reaction that are too high to be of use for fuel cell vehicles. Recent experimental work has focused on destabilizing metal hydrides through alloying with other elements. A very large number of possible destabilized metal hydride reaction schemes exist. The thermodynamic data required to assess the enthalpies of these reactions, however, are not available in many cases. We have used first principles density functional theory calculations to predict the reaction enthalpies for more than 100 destabilization reactions that have not previously been reported. Many of these reactions are predicted not be useful for reversible hydrogen storage, having calculated reaction enthalpies that are either too high or too low. More importantly, our calculations identify five promising reaction schemes that merit experimental study: $3LiNH_2 + 2LiH + Si \rightarrow Li_5N_3Si + 4H_2$, $4LiBH_4 + MgH_2 \rightarrow 4LiH + MgB_4 + 7H_2$, $7LiBH_4 + MgH_2 \rightarrow 7LiH + MgB_7 + 11.5H_2$, $CaH_2 + 6LiBH_4 \rightarrow CaB_6 + 6LiH + 10H_2$, and $LiNH_2 + MgH_2 \rightarrow LiMgN + 2H_2$.

Introduction

The large-scale deployment of vehicular fuel cells is hampered by the absence of a commercially viable hydrogen storage technology. A selection of relatively lightweight, low-cost, and high-capacity hydrogen storage devices must be available in a variety of sizes to meet different energy needs.[1,2] Current long-term U.S. Department of Energy (DOE) guidelines call for a system hydrogen storage density of 9 wt % and a volumetric density of 81 kg H_2/m^3 to enable fuel cell powered vehicles to be able to replace petroleum-fueled vehicles on a large scale.[3−5] In addition to these challenging targets, on-board devices must operate under various other performance constraints. For example, their operating conditions should preferably be below 100 °C and use pressures below about 100 bar. Storage materials that can meet these targets will be useful not only in fuel cell vehicles but also in a range of other applications for hydrogen as a fuel.

Current hydrogen storage materials are unable to meet these storage requirements. For example, high-pressure storage tanks currently in use on prototype fuel cell vehicles do not meet the long-term volumetric and gravimetric density targets. New materials are therefore being investigated, including complex metal hydrides such as alanates, amides, and borohydrides. The hydrides of period 2 and 3 metals have relatively high hydrogen densities but are often thermodynamically very stable and do not typically release hydrogen until temperatures of 250 °C or higher are reached.[6,7] It has been found that using Ti as a catalyst allows reversible storage of 5.6 wt % in $NaAlH_4$.[8−10] Reactions of $LiNH_2$ and LiH to give Li_2NH have also been shown to have a reversible storage capacity of 6.5 wt %.[11,12]

Practical hydrogen storage materials must exhibit favorable thermodynamic properties and have sufficiently rapid kinetics of hydrogen charging and discharging. In this paper, we concentrate exclusively on thermodynamic properties. Kinetics can potentially be improved by control of particle size,[13,14] use of appropriate catalysts,[8] etc. Unfavorable thermodynamics, on the other hand, is most effectively addressed by using a different material for H_2 storage. Although the equilibrium between gaseous H_2 and a metal hydride is determined by both enthalpic and entropic contributions to the system's free energy, enthalpy alone provides a useful means to screen candidate materials.[15] The temperature of dehydrogenation can be reliably estimated by $\Delta H = T\Delta S$, where ΔH and ΔS are the enthalpy and entropy change of the dehydrogenation reaction, respectively. Züttel et al.[16] have argued that the entropic contribution to metal hydride reactions is approximately 130 J K^{-1} mol^{-1} for most simple metal−hydrogen systems. Lower values of ΔS can occur for complex metal hydrides. For example, for $LiBH_4 \rightarrow LiH + B + {}^3/_2H_2$, ΔS is 97 J K^{-1} mol^{-1}.[17] If we estimate that $95 \leq \Delta S \leq 140$ J K^{-1} mol^{-1}, then for the dehydrogenation temperature to lie in the range of 50−150 °C requires that $30 \leq \Delta H \leq 60$ kJ mol/H_2. Reactions with ΔH substantially higher than 60 kJ/mol H_2 will not have appreciable hydrogen pressures until the temperature is unacceptably high. If ΔH is significantly less than 30 kJ/mol H_2, the material will not be easily reversible. Based on this discussion, we pose the task of identifying metal hydrides of interest for reversible H_2 storage as finding systems for which $30 \leq \Delta H \leq 60$ kJ/mol H_2 and that yield significant gravimetric quantities of H_2.

The work of Reilly and Wiswall[18,19] showed that it is possible to modify the thermodynamics of hydrogenation/dehydrogenation reactions by using additives to form compounds or alloys in the dehydrogenated state that are energetically favorable with respect to the products of the reaction without additives. This concept is known as destabilization. Additives added to hydrides

* Corresponding author. E-mail: sholl@andrew.cmu.edu.
[†] Carnegie Mellon University.
[‡] University of Pittsburgh.
[§] National Energy Technology Laboratory.

10.1021/jp060482m CCC: $33.50
Published on Web 04/07/2006

to form compounds with the dehydrogenated metals that are stable with respect to their constituent elements can increase the equilibrium pressure of the dehydrogenation reaction. The principle underlying this concept is that having a stabilized dehydrogenated state reduces ΔH. For example, the partial decomposition of $LiBH_4$ to $LiH + B + {}^3/_2H_2$ can give 13.6 wt % hydrogen, but $\Delta H \approx 69$ kJ/mol H_2 for this reaction,[20] which means that high temperatures are required to release the H_2. Adding MgH_2 to $LiBH_4$ leads to reversible hydrogenation and dehydrogenation of $LiBH_4$ with a considerable reduction in ΔH.[21] In this case, dehydrogenation proceeds as $LiBH_4 + {}^1/_2MgH_2 \leftrightarrow LiH + {}^1/_2MgB_2 + 2H_2$, with a maximum hydrogenation capacity of 11.4 wt %. The MgB_2 formed during the reaction stabilizes the dehydrogenated state and thus destabilizes $LiBH_4$. Destabilization has also been demonstrated for LiH and MgH_2 using Si as an additive to destabilize these hydrides.[22] Si binds with Li and Mg to form stable compounds that reduce the dehydrogenation enthalpies. The concept of destabilization thus relies on being able to identify compounds that can lead to formation of stabilized compounds, thus reducing the enthalpy of the overall reaction and increasing the partial pressure of the hydrides.

The concept underlying the destabilization of metal hydrides is very general, and therefore a large number of potential destabilization reactions exist. The primary obstacle to evaluating the potential utility of many candidate reactions is that information on the heats of formation of the compounds involved in the reactions is not readily available. To address this issue, we have performed first principles density functional theory (DFT) calculations for a large number of potential destabilization schemes. Our calculated results are in good agreement with the reaction enthalpies of destabilization reactions for which this information is available from other sources,[17] suggesting that our DFT calculations can provide quantitative insight into reactions of this type. Our calculations identify multiple reaction schemes that have more favorable enthalpic properties than examples that have been identified in previous experiments. These newly identified destabilization schemes may be of considerable importance in developing robust materials for hydrogen storage.

Computational Details

Plane wave DFT calculations were performed with the Vienna Ab initio Simulation package (VASP).[23,24] The calculations examine a spatially infinite material using periodic boundary conditions in all the principal directions. We have used both ultrasoft pseudopotentials (USPP) and the projector augmented wave (PAW) method[25] for prediction of reaction enthalpies. Electron exchange and correlation effects were described using the generalized gradient approximation (GGA) with the Perdew−Wang 91 (PW91) functional.[26] We have performed test calculations with the USPP revised Perdew−Burke−Ernzerhof[27] and PAW Perdew−Burke−Ernzerhof[28] functionals, but these resulted in ΔH values that were much lower than experimental or PW91 values. The bond energy of H_2 is key to the accuracy of all the ΔH calculations. We have therefore computed the bond energy of H_2 from USPP−PW91 and PAW−PW91; both methods give 4.56 eV, which is in good agreement with the experimental value of 4.52 eV.[29] Most of the unit cells calculations were performed with a Monkhorst−Pack mesh of $9 \times 9 \times 9$ *k*-points. A smaller number of *k*-points was used for a few systems having the largest unit cells. Convergence of the energies with the number of *k*-points was checked for several test reactions. The results of these test calculations are given in the Supporting Information, Tables S1−S3. Calculations using different functionals are also presented in Tables S1−S3. Geometry optimizations for bulk structures were performed by allowing all atomic positions and all cell parameters to vary. Geometric relaxations were carried out using a conjugate gradient algorithm until the forces on each of the unconstrained atoms were less than 0.03 eV/Å. For total energy calculations for reactions involving Li/B/N or their compounds, the energy cutoffs for all compounds were 260/265/375 eV for USPP and 260/325/425 for PAW calculations. For all other reactions the energy cutoffs were 210 eV for USPP and 260 eV for PAW calculations. The effect of energy cutoff on ΔH for several test reactions has been computed, and the results are given in Tables S4−S6 in the Supporting Information. The initial geometry optimizations were performed using an energy cutoff 30% larger than the cutoff for the final total energy calculations to obtain a reliable stress tensor for VASP calculations.

The enthalpy of the reaction at 0 K was calculated using

$$\Delta H = \sum_{\text{products}} E - \sum_{\text{reactants}} E \qquad (1)$$

where E is the total energy of one of the bulk structures of interest as calculated by DFT. We have not accounted for zero-point corrections in any of the total energies. The heats of formation for all the compounds we have considered are listed in the Supporting Information.

Our calculations included 49 compounds. For the majority of the compounds we examined, the initial structures for geometry relaxations were obtained from the tabulated experimental data available from Wyckoff,[30] Pearson's handbook,[31] and the ICSD database.[32] Four compounds require special comment. First, to the best of our knowledge, no complete experimental structural information is available for $Ca(AlH_4)_2$. We have therefore used the structure predicted recently by Løvvik from DFT optimization of structures based on similar compounds.[33] Second, Li_5N_3Si is reported to have 10.67 formula units in the crystallographic unit cell, with the Li and Si atoms distributed on the same sites with fractional occupancy.[31] Performing a DFT calculation with this precise stoichiometry of the bulk material is unwieldy, since it would require a supercell with 288 atoms. Instead of performing this very large calculation, we used two separate calculations with unit cells containing $Li_{54}N_{32}Si_{10}$ and $Li_{53}N_{32}Si_{11}$. In each case, the Si atoms were distributed randomly among the available sites in the crystallographic unit cell. Third, the compound nominally referred to as MgB_7 actually exists in an orthorhombic form with a composition of $Mg_{0.97}B_7$ and eight formula units in the unit cell.[34] As with Li_5N_3Si, performing a plane wave calculation with the exact stoichiometry is not feasible, and hence we have performed calculations with Mg_8B_{56}, the nominal stoichiometric compound, and Mg_7B_{56}. The latter structure was formed by removing one Mg atom from the unit cell defined by the nominal stoichiometric compound. Fourth, $LiBH_4$ exists in an orthorhombic crystal structure at room temperature but undergoes a structural transition to form a hexagonal phase above 384 K.[35] This structural transition lies in the operating temperature range of interest to us, so we performed calculations with both of these polymorphs.

Results

The calculated lattice parameters for the 49 materials considered in this work are presented in Table 1, along with experimental structural data; the agreement is generally very good, as expected.

TABLE 1: Comparison of the Experimental and the DFT Calculated (USPP−GGA) Structural Parameters for the Compounds in the Reactions Studied, with All Distances in angstroms and Angles in degrees[a]

		structural parameters (Å)	
compound	space group	experimental[b]	calculated
Al	$Fm\bar{3}m$	$a = 4.049$	$a = 4.049$
$Al_{12}Mg_{17}$	$I\bar{4}3m$	$a = 10.524$	$a = 10.544$
Al_2Ca	$Fd\bar{3}m$	$a = 8.035$	$a = 7.994$
$Al_2Ca_3Si_2$	$Immm$	$a = 4.000$, $b = 18.240$ $c = 4.576$	$a = 4.076$, $b = 18.438$ $c = 4.515$
Al_2CaSi_2	$P\bar{3}m1$	$a = 4.130$, $c = 7.145$	$a = 4.147$, $c = 7.063$
Al_2Li_3	$R\bar{3}\underline{m}$	$a = 4.508$, $c = 14.259$	$a = 4.429$, $c = 13.961$
Al_3Li	$Pm\bar{3}m$	$a = 4.01$	$a = 4.013$
Al_4Li_9	$C2/m$	$a = 19.1551$, $b = 4.4988$ $c = 5.4288$, $\beta = 107.361$	$a = 18.69$, $b = 4.44$ $c = 5.27$, $\beta = 107.34$
AlB_2	$P6/mmm$	$a = 3.009$, $c = 3.262$	$a = 3.004$, $c = 3.292$
AlH_3	$R\bar{3}\underline{c}$	$a = 4.227$, $c = 11.244$	$a = 4.426$, $c = 11.851$
AlLi	$Fd\bar{3}m$	$a = 6.3757$	$a = 6.326$
$AlLi_3N_2$	$Ia\bar{3}$	$a = 9.461$	$a = 9.440$
AlLiSi	$F\bar{4}3m$	$a = 5.928$	$a = 5.923$
AlN	$P6_3mc$	$a = 3.11$, $c = 4.98$	$a = 3.12$, $c = 4.998$
B	$R\bar{3}m$	$a = 4.908$, $c = 12.559$	$a = 4.890$, $c = 12.496$
Ca	$Fm\bar{3}m$	$a = 5.588$	$a = 5.499$
$Ca(AlH_4)_2$	$Pbca$	$a = 13.37$, $b = 9.28$ $c = 8.91$[c]	$a = 13.29$, $b = 9.456$ $c = 8.97$
Ca_2LiSi_3	$Pnnm$	$a = 11.24$, $b = 10.50$ $c = 4.39$	$a = 11.165$, $b = 10.479$ $c = 4.353$
Ca_3BN_3	$P4/mmm$	$a = 3.5494$, $c = 8.2136$	$a = 3.519$, $c = 8.174$
Ca_5Si_3	$I4/mcm$	$a = 7.64$, $c = 14.62$	$a = 7.601$, $c = 14.741$
Ca_2N	$R\bar{3}\underline{m}$	$a = 3.638$, $c = 18.78$	$a = 3.611$, $c = 18.852$
CaB_6	$Pm\bar{3}m$	$a = 4.145$	$a = 4.129$
CaH_2	$Pnma$	$a = 5.925$, $b = 3.60$ $c = 6.838$	$a = 5.858$, $b = 3.546$ $c = 6.699$
$CaLi_2$	$P6_3/mmc$	$a = 6.268$, $c = 10.219$	$a = 6.126$, $c = 9.984$
$CaLiSi_2$	$Pnma$	$a = 7.98$, $b = 3.80$ $c = 10.69$	$a = 7.876$, $b = 3.799$ $c = 10.576$
CaMgSi	$Pnma$	$a = 7.48$, $b = 4.40$ $c = 8.29$	$a = 7.455$, $b = 4.409$ $c = 8.300$
$CaMg_2$	$P6_3/mmc$	$a = 6.225$, $c = 10.18$	$a = 6.226$, $c = 10.050$
CaSi	$Cmcm$	$a = 4.559$, $b = 10.731$ $c = 3.890$	$a = 4.528$, $b = 10.674$ $c = 3.882$
Li	$Im\bar{3}m$	$a = 3.510$	$a = 3.407$
$Li_{12}Mg_3Si_4$	$I\bar{4}3d$	$a = 10.688$	$a = 10.601$
Li_3BN_2	$P4_2/mnm$	$a = 4.644$, $c = 5.259$	$a = 4.621$, $c = 5.226$
Li_3N	$P6_3/mmc$	$a = 3.552$, $c = 6.311$	$a = 3.505$, $c = 6.256$
Li_5N_3Si (10 Si atoms)	$Ia\bar{3}$	$a = 9.436$	$a = 9.435$
Li_5N_3Si (11 Si atoms)	$Ia\bar{3}$	$a = 9.436$	$a = 9.43$, $b = 9.42$ $c = 9.42$
$LiBH_4$	$Pnma$	$a = 7.173$, $b = 4.434$ $c = 6.798$	$a = 7.133$, $b = 4.325$ $c = 6.574$
$LiBH_4$	$P6_3mc$	$a = 4.276$, $c = 6.948$	$a = 4.172$, $c = 7.259$
LiH	$Fm\bar{3}m$	$a = 4.085$	$a = 3.942$
LiMgN	$Pnma$	$a = 7.1586$, $b = 3.5069$ $c = 5.0142$	$a = 7.163$, $b = 3.481$ $c = 4.989$
LiN_3	$C2/m$	$a = 5.627$, $b = 3.319$ $c = 4.979$, $\beta = 107.4$	$a = 5.628$, $b = 3.319$ $c = 5.007$, $\beta = 107.13$
$LiNH_2$	$I\bar{4}$	$a = 5.037$, $c = 10.278$	$a = 4.990$, $c = 10.234$
Mg	$P6_3/mmc$	$a = 3.209$, $c = 5.210$	$a = 3.197$, $c = 5.188$
Mg_2Si	$Fm\bar{3}m$	$a = 6.390$	$a = 6.361$
Mg_3BN_3	$P6_3/mmc$	$a = 3.5445$, $c = 16.0353$	$a = 3.537$, $c = 16.149$
Mg_3N_2	$Ia\bar{3}$	$a = 9.972$	$a = 9.970$
MgB_2	$P6/mmm$	$a = 3.084$, $c = 3.522$	$a = 3.068$, $c = 3.520$
MgB_4	$Pnma$	$a = 5.464$, $b = 4.428$ $c = 7.472$	$a = 5.454$, $b = 4.379$ $c = 7.421$
MgB_7 (Mg_8B_{56})	$Imma$	$a = 5.970$, $b = 10.480$ $c = 8.125$	$a = 5.949$, $b = 10.438$ $c = 8.092$
MgB_7 (Mg_7B_{56})	$Imma$	$a = 5.970$, $b = 10.480$ $c = 8.125$	$a = 5.944$, $b = 10.461$ $c = 8.104$
MgH_2	$P4_2/mnm$	$a = 4.517$, $c = 3.021$	$a = 4.466$, $c = 2.992$
MgN_2Si	$Pna2_1$	$a = 5.2725$, $b = 6.4733$ $c = 4.9862$	$a = 5.925$, $b = 6.468$ $c = 5.010$
Si	$Fd\bar{3}m$	$a = 5.430$	$a = 5.460$
SiB_6	$Pm3m$	$a = 4.15$	$a = 4.14$

[a] For $Ca(AlH_4)_2$, we compare our results with the previous DFT calculations of Løvvik (ref 33). [b] Refs 30−32. [c] Ref 33.

TABLE 2: Reaction Enthalpies from DFT Calculations Compared with Values Obtained from Thermodynamic Tables (ref 17) and Experiments[a]

reaction	wt % H_2	ΔH (tabulated)	ΔH (exptl)	ΔH (USPP)	ΔH (PAW)
$MgH_2 + 2LiBH_4 \rightarrow 2LiH + MgB_2 + 4H_2$	11.56	45.96		64.6	66.8
$2MgH_2 + Si \rightarrow Mg_2Si + 2H_2$	5.00	37.24		37.1	37.9
$2LiH \rightarrow 2Li + H_2$	12.70	181.26	180.4[b]	174.0	172.5
$MgH_2 \rightarrow Mg + H_2$	7.67	76.15	70.6[b]	64.1	65.1
$LiBH_4 \rightarrow LiH + B + 1.5H_2$	13.91	66.55	68.9[c]	79.6	82.4

[a] ΔH values are listed in kJ/mol H_2. [b] Ref 29. [c] Ref 20.

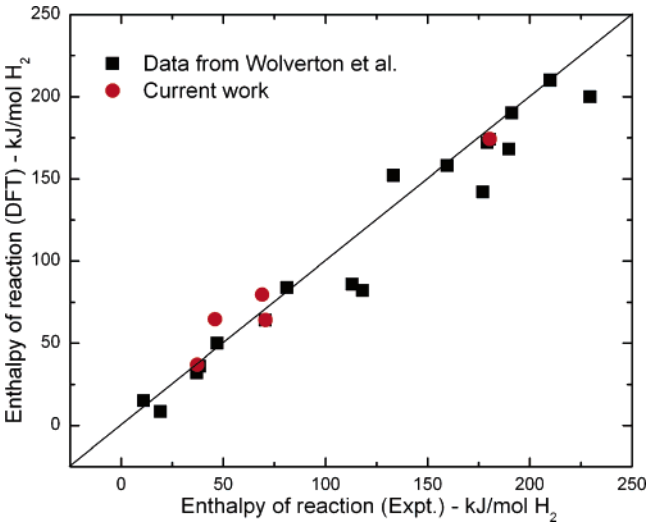

Figure 1. Comparison of data from experiments or thermodynamic tables for hydride decomposition enthalpies with plane wave DFT predictions. All ΔH values are in kJ/mol H_2. The results shown with black squares are from Wolverton et al. (ref 36).

TABLE 3: Reaction Enthalpies from Our DFT Calculations Compared with Values Obtained Using DFT by Other Researchers[a]

reaction	ΔH (other sources)	ΔH (USPP)	ΔH (PAW)
$CaH_2 \rightarrow Ca + H_2$	181.5[b]	180.3	175.2
$2AlH_3 \rightarrow 2Al + 3H_2$	10.04[c]	10.8	11.1
$Ca(AlH_4)_2 \rightarrow 2Al + CaH_2 + 3H_2$	12.5[d]	12.2	13.9
$LiBH_4 \rightarrow LiH + B + 1.5H_2$	71.3[e],75[f]	79.6 (o)	82.4 (o)
		68.7 (h)	71.5 (h)
$LiNH_2 + 2LiH \rightarrow Li_3N + 2H_2$	99[g]	103.4	109.4
$LiBH_4 + 2LiNH_2 \rightarrow Li_3BN_2 + 4H_2$	23[g]	21.9 (o)	24.3 (o)
		17.8 (h)	20.2 (h)

[a] ΔH values are listed in kJ/mol H_2. The enthalpy for the reaction with the hexagonal and orthorhombic polymorphs of $LiBH_4$ is denoted by (h) and (o), respectively. [b] Ref 47. [c] Ref 36. [d] Ref 33. [e] Ref 48. [f] Ref 49. [g] Ref 38.

The first aim of our calculations was to assess the accuracy of DFT for computing reaction enthalpies for destabilization reactions. We therefore initially considered reactions for which the enthalpy of formation for all the participating species is available from thermodynamic tables.[17] Table 2 lists five reactions of this type, including three direct metal hydride reactions and two destabilized reactions. For these five reactions, the tabulated entropy change for the reaction varies from 97 to 149 J K^{-1} mol^{-1}, in reasonable agreement with the range we used above to place bounds on the desirable enthalpy range for the dehydrogenation reactions. The two destabilized reactions listed in Table 2 have reaction enthalpies that are within the range appropriate for practical use. These two reactions have been studied experimentally by Vajo and co-workers.[21,22] It can be seen from Table 2 that there are only minor differences between the USPP and PAW DFT calculations. There are considerable quantitative discrepancies that arise when the DFT results are compared with the tabulated or experimental data. Within the USPP calculations, the DFT result varies from overpredicting the reaction enthalpy by 18.6 kJ/mol H_2 for the first reaction in the table to underpredicting the enthalpy by 12 kJ/mol H_2 for the decomposition of MgH_2.

A more detailed examination of this issue is possible by adding our calculations to the large set of direct decomposition reactions for metal hydrides that were examined with plane wave GGA−DFT calculations by Wolverton et al.[36] The approach we have taken in our calculations is essentially identical to that of Wolverton et al., so it is entirely appropriate to combine these two sets of calculations in order to discuss their accuracy. Figure 1 shows the experimental (or tabulated) and DFT-predicted reaction enthalpies for 21 metal hydride dehydrogenation reactions. The average value of $\Delta H_{DFT} - \Delta H_{exptl}$ is −6.3 kJ/mol H_2, and the standard deviation in this quantity is 14.9 kJ/mol H_2. It is clear from these results that the DFT calculations cannot be used to make precise predictions (say, within 10 kJ/mol H_2) of the reaction enthalpies. We claim, however, that DFT calculations are sufficiently accurate to identify potential destabilization schemes of interest. Recall that our aim is to find reactions for which $30 \leq \Delta H \leq 60$ kJ/mol H_2. The DFT results shown in Figure 1 are clearly able to distinguish the small number of reactions that either satisfy this condition (or come close to satisfying it) from the larger collection of reactions that lie far from these limits. Said differently, if only the DFT data from Figure 1 were available, it would have been straightforward to identify the small number of candidates that warranted experimental study to precisely establish their reaction enthalpies. Below, we use our DFT calculations to predict reaction enthalpies for a large number of potential destabilization schemes with the aim of identifying the small number of schemes that have promising reaction thermodynamics. We emphasize that the primary motivation of our calculations is to motivate experimental studies of the most promising materials and to reduce unnecessary experimental studies of materials whose thermodynamics are demonstrably unpromising.

Before moving on to our main results, we briefly comment on the level of agreement between our calculations and similar DFT calculations in earlier studies. Table 3 shows a comparison of our results with earlier DFT calculations by other researchers. As should be expected, there is excellent agreement between these results. In most cases, earlier studies applied DFT calculations to one or a small number of metal hydride reactions. The results shown from previous calculations with $LiBH_4$ in Table 3 are all for the orthorhombic crystal structure.

The list of materials given in Table 1 enabled us to compute reaction enthalpies for 129 new reactions for which these enthalpies were not previously known (data included in the Supporting Information). Figure 2 shows the plot of the reaction

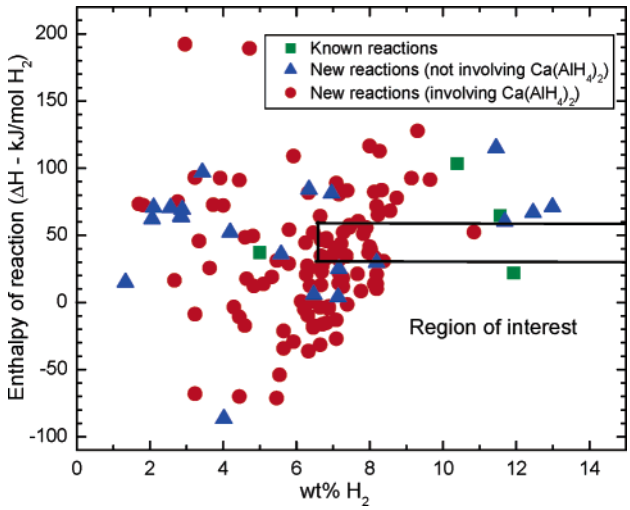

Figure 2. USPP−DFT predictions of ΔH for 129 new destabilized reactions along with 4 known ones. The region of interest includes reactions which have >6.5 wt % H_2 and reaction enthalpies between 30 and 60 kJ/mol H_2.

enthalpies as a function of the wt % of H_2 that can be obtained from a particular reaction assuming the dehydrogenation reaction goes to completion. It is immediately clear that many of these reactions are uninteresting from the point of view of hydrogen storage for either thermodynamic or gravimetric reasons (or both).

We identify promising candidate reaction schemes by considering each of the reactions shown in Figure 2 that have $15 \leq \Delta H \leq 75$ kJ/mol H_2 and that yield >6.5 wt % H storage. We initially exclude reactions that we know can proceed by a lower reaction enthalpy pathway, as discussed below for reactions involving $Ca(AlH_4)_2$. We have chosen the value of 6.5 wt % because it is slightly larger than the interim 2010 DOE targets.[3] The range of enthalpies is chosen so that after accounting for the uncertainty associated with our DFT calculations we will capture essentially all reactions that can satisfy the experimental bounds of $30 \leq \Delta H \leq 60$ kJ/mol H_2. That is, we identify candidate reactions in an inclusive manner, consistent with our goal of motivating detailed experimental studies of potential candidates. While recognizing that this inclusive approach may yield some false positives, we feel it is more productive to list all the reactions identified in this way in detail rather than exclude examples that might be rejected by a more conservative approach. We reiterate that the reaction enthalpies of all the reactions we have considered are listed in the Supporting Information, so readers who prefer to apply a different screening criterion than the one we have suggested can readily do so.

Our inclusive criterion for identifying interesting reaction schemes yields seven reactions. One is the reaction already studied experimentally by Vajo et al.[21]

$$2LiBH_4 + MgH_2 \rightarrow MgB_2 + 2LiH + 4H_2 \qquad (2)$$

This reaction can yield a maximum of 11.56 wt % H at completion and has been demonstrated experimentally to yield >9 wt % H reversibly. A second reaction is the one suggested recently by Pinkerton et al.[37] and also by Aoki et al.:[38]

$$LiBH_4 + 2LiNH_2 \rightarrow Li_3BN_2 + 4H_2 \qquad (3)$$

This reaction yields 11.9 wt % H at completion and is predicted by DFT to have $\Delta H = 22$ (24) kJ/mol H_2 using the USPP (PAW) approach and the orthorhombic form of $LiBH_4$. Pinkerton et al. found that ball milling or heating the $LiBH_4 + 2LiNH_2$ mixture causes it to react to form a new quaternary hydride phase with the approximate composition $Li_3BN_2H_8$. X-ray diffraction patterns indicate the new phase is a body-centered cubic structure with a lattice constant of $a = 10.76$ Å. The quaternary phase released about 11.5% H between about 523 and 623 K. Aoki et al. used USPP−GGA calculations to predict the enthalpy of dehydrogenation for the above reaction to be 23 kJ/mol H_2. They also carried out $p-c$ isotherm measurements on the ball-milled mixture of $LiBH_4$ and $LiNH_2$ to obtain the dehydrogenation curves at 522 K. At this temperature 7.8 wt % H was desorbed, corresponding to 66% of the total possible yield. From these two studies it is apparent that the reaction pathway identified in (3) does not directly occur because of the formation of an intermediate quaternary hydride phase, $Li_3BN_2H_8$. It appears that the quaternary phase is metastable with respect to the reactants and products, given that the dehydrogenation of $Li_3BN_2H_8$ is apparently exothermic.

Crucially, our approach also identifies five interesting reactions that have not previously been proposed or examined. All of these examples are summarized in Table 4. One example is

$$3LiNH_2 + 2LiH + Si \rightarrow Li_5N_3Si + 4H_2 \qquad (4)$$

This reaction yields 7.16 wt % H on completion. Our DFT calculations predict that the reaction enthalpy is 19−30 (23−34) kJ/mol H_2 using the USPP (PAW) approach. The range of values for this reaction reflects the variants in the Li_5N_3Si crystal structure that were employed in our calculations (see the Computational Details). A related reaction involves a mixture of $LiNH_2$ and MgH_2:

$$LiNH_2 + MgH_2 \rightarrow LiMgN + 2H_2 \qquad (5)$$

This reaction releases 8.19 wt % H on completion, with a DFT-predicted reaction enthalpy of 29.7 (31.9) kJ/mol H_2 using the USPP (PAW) approach.

A similar reaction to (5) has been studied by Luo,[39] who investigated the dehydrogenation characteristics of a mixture of $LiNH_2$ and MgH_2. It was thought that as the mixture of $LiNH_2 + LiH$ reacts to form $Li_2NH + H_2$, the mixture of $LiNH_2$ and MgH_2 in the molar ratio of 2:1 would react to form Li_2NH, MgNH, and H_2 as products, probably with better sorption characteristics. This mixture was indeed shown to have significantly better sorption characteristics than a mixture of $LiNH_2$ and LiH. Luo observed that nearly 90% of the total hydrogen for the predicted reaction $2LiNH_2 + MgH_2 \rightarrow Li_2NH + MgNH + 2H_2$ was released during the first 0.5 h at a temperature of 220 °C. Also, the decomposition enthalpy for the $2LiNH_2 + MgH_2$ mixture was found to be 34 kJ/mol of H_2 as compared to 51 kJ/mol for the $LiNH_2-LiH$ mixture. It was initially thought that similar to the $LiNH_2 + LiH$ case the products should contain Li_2NH and MgNH. But the X-ray diffraction pattern of the dehydrogenated sample consisted of no trace of either Li_2NH or MgNH, and it was suggested that the reaction proceeds as $2LiNH_2 + MgH_2 \rightarrow Li_2MgN_2H_2 + 2H_2$. Further studies by Luo and Sickafoose[40] revealed that the rehydrided product in the above reaction is not $2LiNH_2 + MgH_2$ but $Mg(NH_2)_2 + 2LiH$. Powder XRD was used to identify the phases during the reaction, and it was observed that the conversion of $2LiNH_2 + MgH_2$ to $Mg(NH_2)_2 + 2LiH$ takes place during heating at 220 °C.

TABLE 4: Reactions with $15 \leq \Delta H \leq 75$ kJ/mol H_2 and Gravimetric Densities >6.5 wt % (Not Involving $Ca(AlH_4)_2$)[a]

reaction	wt % H_2	ΔH (USPP)	ΔH (PAW)
$MgH_2 + 2LiBH_4 \rightarrow 2LiH + MgB_2 + 4H_2$	11.56	64.6 (o) 56.4 (h)	66.8 (o) 58.6 (h)
$LiBH_4 + 2LiNH_2 \rightarrow Li_3BN_2 + 4H_2$	11.9	21.9 (o) 17.8 (h)	24.3 (o) 20.2 (h)
$3LiNH_2 + 2LiH + Si \rightarrow Li_5N_3Si + 4H_2$ (10/11 Si atoms)	7.16	29.8/19.2[b]	34.2/23.3[b]
$4LiBH_4 + MgH_2 \rightarrow 4LiH + MgB_4 + 7H_2$	12.46	66.8 (o) 57.5 (h)	69.2 (o) 59.9 (h)
$7LiBH_4 + MgH_2 \rightarrow 7LiH + MgB_7 + 11.5H_2$	12.99	69.2−73.1 (o) 59.2−63.1 (h)	71.5−75.5 (o) 61.5−65.5 (h)
$CaH_2 + 6LiBH_4 \rightarrow CaB_6 + 6LiH + 10H_2$	11.69	60.3 (o) 50.4 (h)	62.7 (o) 52.9 (h)
$LiNH_2 + MgH_2 \rightarrow LiMgN + 2H_2$	8.19	29.7	31.9

[a] For reactions involving $LiBH_4$, the enthalpy for the reaction with the hexagonal and orthorhombic polymorphs of $LiBH_4$ is denoted by (h) and (o), respectively. [b] Indicates results for final materials with varying Si loading.

TABLE 5: Reactions Involving $Ca(AlH_4)_2$ that Have Reaction Enthalpies between 15 and 40 kJ/mol H_2 and Can Release More than 6.5 wt % H_2

reaction	wt % H_2	ΔH (USPP)	ΔH (PAW)
$3Ca(AlH_4)_2 + 2Si \rightarrow 2Al_2Ca + Al_2CaSi_2 + 12H_2$	6.69	23.0	24.1
$3Ca(AlH_4)_2 + 2Si \rightarrow 4Al + Al_2Ca_3Si_2 + 12H_2$	6.69	27.6	28.4
$6Ca(AlH_4)_2 + 17MgH_2 \rightarrow Al_{12}Mg_{17} + 6CaH_2 + 35H_2$	6.67	34.6	35.4
$Ca(AlH_4)_2 + 2LiH \rightarrow 2AlLi + CaH_2 + 4H_2$	6.85	33.3	33.3
$3Ca(AlH_4)_2 + 4LiH \rightarrow 4AlLi + Al_2Ca + 2CaH_2 + 12H_2$	7.17	31.8	31.8

An interesting observation was that other researchers who have studied the $Mg(NH_2)_2$ and LiH system have obtained different products depending upon the starting stoichiometry of the reactants, e.g., Nakamori et al.[41] studied $Mg(NH_2)_2 + 4LiH \rightarrow {}^1/_3Mg_3N_2 + {}^4/_3Li_3N + 4H_2$ and $Mg(NH_2)_2 + {}^8/_3LiH \rightarrow {}^1/_3Mg_3N_2 + {}^4/_3Li_2NH + {}^8/_3H_2$ has been studied by Leng et al.[42] and Ichikawa et al.[43] Nakamori et al.[41] have observed that increasing the LiH content in the mixture is an effective way to prevent ammonia release; however, the trade off is that the amount of desorbed hydrogen is reduced. The observation that changing the molar ratios of the reactants gives rise to different products lends credence to our prediction that LiMgN may be obtained as a product of $LiNH_2$ and MgH_2, as given in (5) and also justifies the reactions given below in reactions (6) and (7).

Two other examples identified by our calculations are variants of (2):

$$4LiBH_4 + MgH_2 \rightarrow MgB_4 + 4LiH + 7H_2 \quad (6)$$

$$7LiBH_4 + MgH_2 \rightarrow MgB_7 + 7LiH + 11.5H_2 \quad (7)$$

These schemes differs from reaction (2) by including larger amounts of $LiBH_4$ as a reactant, forming MgB_4 or MgB_7 as a product rather than MgB_2. Reactions (6) and (7) release 12.5 and 13 wt % H on completion. Our USPP−DFT calculations predict a reaction enthalpy of 66.8 (69.2−73.1) kJ/mol H_2 using the orthorhombic form of $LiBH_4$ for the reaction forming MgB_4 (MgB_7). The range of enthalpies for the latter reaction is due to the different structures of MgB_7 used to account for the vacancies in the crystal structure.

The fifth example involves CaH_2:

$$CaH_2 + 6LiBH_4 \rightarrow CaB_6 + 6LiH + 10H_2 \quad (8)$$

Upon completion, this reaction releases 11.7 wt % H, and the DFT-predicted reaction enthalpy is 60 (63) with USPP (PAW).

Several of the promising reactions listed above include $LiBH_4$ as a reactant. $LiBH_4$ is known to undergo a structural transformation from an orthorhombic to a hexagonal form at 384 K.[35] DFT correctly predicts that the orthorhombic form is the more stable low-temperature structure. When the reaction enthalpies of interest are recomputed with the hexagonal $LiBH_4$ structure only relatively minor changes in the predicted reaction enthalpies appear (see Table 4). A detailed treatment of the interplay between these two structural forms in each of the reactions of interest would require calculation or measurement of the entropic contributions to each phase, a task that is beyond the scope of our present work.

Many of the new reactions shown in Figure 2 involve $Ca(AlH_4)_2$. The USPP (PAW)-predicted DFT reaction enthalpy for the decomposition of $Ca(AlH_4)_2$ via

$$Ca(AlH_4)_2 \rightarrow CaH_2 + 2Al + 3H_2 \quad (9)$$

is only 12 (14) kJ/mol H_2. Thus, even though many reactions with superficially attractive reaction enthalpies can be constructed using $Ca(AlH_4)_2$, they are all likely to be metastable pathways with respect to the direct decomposition reaction. Only limited experimental data are available for $Ca(AlH_4)_2$, but it is interesting to note that decomposition of this compound is not reported to take place until temperatures in excess of 200 °C are reached.[44] This high decomposition temperature suggests that the decomposition of $Ca(AlH_4)_2$ is kinetically rather than thermodynamically limited, even allowing for uncertainties in the DFT-predicted reaction enthalpy. If reaction 9 is kinetically limited, it is at least conceivable that more facile reaction pathways with slightly higher reaction enthalpies may exist and therefore be experimentally observable. This rather speculative concept indicates that it is at least worthwhile identifying a number of these metastable reactions. Table 5 presents a list of reactions involving $Ca(AlH_4)_2$ that have reaction enthalpies in the range of 15−40 kJ/mol H_2 and release more than 6.5 wt % H_2 on completion. We reiterate that on purely thermodynamic grounds we do not expect these reactions to be observable, unlike the examples in Table 4. Nevertheless, experiments with the materials listed in Table 5 have at least a small probability of identifying interesting metastable reactions.

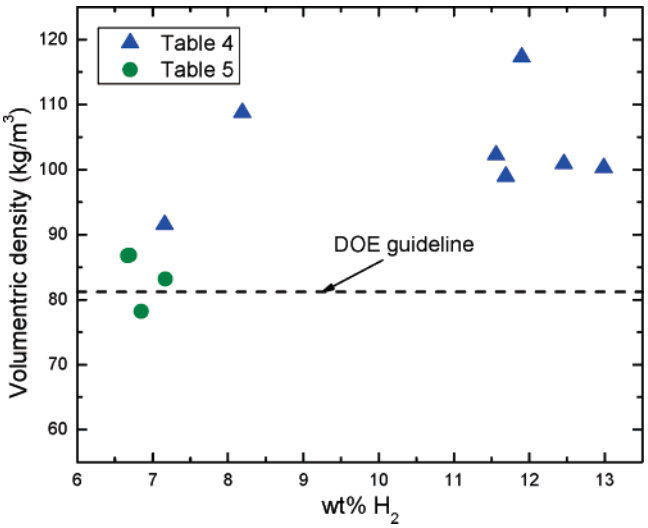

Figure 3. Volumetric storage density for the reactions shown in Tables 4 and 5.

Discussion and Conclusions

We have used plane wave DFT calculations to examine the potential utility for hydrogen storage of a large set of destabilized metal hydride reactions for which thermodynamic data were previously unavailable. Our DFT calculations predict the 0 K reaction enthalpies and do not take zero-point energies into account. More accurate predictions of reaction enthalpies could include calculations for zero-point energy effects and for the specific heats of the compounds of interest. Despite these caveats, comparisons of DFT calculations by us and others indicate that the predictions of these calculations are sufficiently accurate to identify reactions that have favorable properties for reversible hydrogen storage.

Our calculations have identified a number of reactions that have very promising properties in terms of both their reaction enthalpies and their hydrogen storage capacity. These reactions have favorable gravimetric and volumetric hydrogen storage capacities, as shown in Figure 3. Figure 3 also shows the most aggressive DOE guideline to date for volumetric storage.[3] All of the reactions listed in Table 4 exceed this guideline, provided that they go to completion.

Our results suggest two obvious directions for future work. Most importantly, we hope our predictions spur experimental studies of the new destabilization schemes we have identified. The reactions we have identified significantly expand the number of promising destabilization schemes for reversible hydrogen storage that have been suggested. Experimental studies are the only route to definitively answering questions related to the accuracy of our calculations and the kinetics of the dehydrogenation and hydrogenation reactions.

As discussed in the Introduction, the reaction enthalpy provides a useful parameter for screening potential reaction schemes for reversible hydrogen storage. A more complete characterization for reactions for hydrogen storage applications would involve the calculation of free energy change (ΔG) for the reaction. As we have seen above, the enthalpic part of free energy can be calculated efficiently using DFT, and thus a second direction for future work would be to use theoretical methods to quantify the entropic contribution to the most promising reactions. Neglecting entropic contributions is of course not always accurate. For example, Ozolinš et al. have shown recently that vibrational entropy contributions alter the solubility of Si in Al by an order of magnitude.[45] Although entropic contributions can be assessed with DFT calculations,[45,46] the computational effort required to do so is much greater than for the calculations we have reported here, particularly for materials with many atoms in their unit cell. It will clearly be worthwhile in the future to perform calculations of this type for the most promising materials we have identified.

Acknowledgment. This work was supported by the DOE Grant No. DE-FC36-05G015066 and performed in conjunction with the DOE Metal Hydride Center of Excellence. J.K.J. and D.S.S. are NETL Faculty Fellows.

Supporting Information Available: Tables showing the reaction enthalpies of all of the reactions we have considered and the heats of formation for all of the compounds we have considered. This material is available free of charge via the Internet at http://pubs.acs.org.

References and Notes

(1) Schlapbach, L.; Züttel, A. *Nature* **2001**, *414*, 353.
(2) Züttel, A. *Mater. Today* **2003**, *6*, 24.
(3) DOE Hydrogen Storage Targets. http://www.eere.energy.gov/hydrogenandfuelcells/mypp/pdfs/storage.pdf.
(4) *A Multiyear Plan for the Hydrogen R&D Program: Rationale, Structure, and Technology Road Maps*; U.S. Department of Energy. http://www.eere.energy.gov/hydrogenandfuelcells/pdfs/bk28424.pdf, 1999; p 32.
(5) *National Hydrogen Energy Road Map*; U.S. Department of Energy. http://www.eere.energy.gov/hydrogenandfuelcells/pdfs/hydrogen_posture_plan.pdf, 2002; p 17.
(6) Sangster, J.; Pelton, A. D. In *Phase Diagrams of Binary Hydrogen Alloys*; ASM International: Materials Park, OH, 2000.
(7) IEA/DOE/SNL. Hydride Databases Available at Hydride Information Center, Sandia National Laboratories. http://hydpark.ca.sandia.gov.
(8) Bogdanovíc, B.; Schwickardi, M. *J. Alloys Compd.* **1997**, *253*−*254*, 1.
(9) Løvvik, O. M.; Opalka, S. M. *Phys. Rev. B* **2005**, *71*, 054103.
(10) Luo, W.; Gross, K. J. *J. Alloys Compd.* **2004**, *385*, 224.
(11) Chen, P.; Xiong, Z.; Luo, J.; Lin, J.; Tan, K. L. *J. Phys. Chem. B* **2003**, *107*, 10967.
(12) Chen, P.; Xiong, Z.; Luo, J.; Lin, J.; Tan, K. L. *Nature* **2002**, *420*, 302.
(13) Bouaricha, S.; Dodelet, J.-P.; Guay, D.; Huot, J.; Schulz, R. *J. Mater. Res.* **2001**, *16*, 2893.
(14) Huot, J.; Liang, G.; Schulz, R. *Appl. Phys. A* **2001**, *72*, 187.
(15) Grochala, W.; Edwards, P. P. *Chem. Rev.* **2004**, *104*, 1283.
(16) Züttel, A.; Wenger, P.; Rentsch, S.; Sudan, P.; Mauron, P.; Emmenegger, C. *J. Power Sources* **2003**, *118*, 1.
(17) *NIST Chemistry Webbook, NIST Standard Reference Database Number 69*; Linstrom, P. J., Mallard, W. G., Eds.; National Institute of Standards and Technology: Gaithersburg, MD, 2005.
(18) Reilly, J. J.; Wiswall, R. H. *Inorg. Chem.* **1967**, *6*, 2220.
(19) Reilly, J. J.; Wiswall, R. H. *Inorg. Chem.* **1968**, *7*, 2254.
(20) Smith, M. B.; Bass, G. E. *J. Chem. Eng. Data* **1963**, *8*, 342.
(21) Vajo, J. J.; Skeith, S. L.; Meters, F. *J. Phys. Chem. B* **2005**, *109*, 3719.
(22) Vajo, J. J.; Mertens, F.; Ahn, C. C.; Bowman, R. C., Jr.; Fultz, B. *J. Phys. Chem. B* **2004**, *108*, 13977.
(23) Kresse, G.; Hafner, J. *Phys. Rev. B* **1993**, *47*, 558.
(24) Kresse, G.; Furthmüller, J. *Phys. Rev. B* **1996**, *54*, 11169.
(25) Kresse, G.; Joubert, D. *Phys. Rev. B* **1999**, *59*, 1758.
(26) Perdew, J. P.; Chevary, J. A.; Vosko, S. H.; Jackson, K. A.; Pederson, M. R.; Singh, D. J.; Fiolhais, C. *Phys. Rev. B* **1992**, *46*, 6671.
(27) Hammer, B.; Hansen, L. B.; Nørskov, J. K. *Phys. Rev. B* **1999**, *59*, 7413.
(28) Perdew, J. P.; Burke, K.; Ernzerhof, M. *Phys. Rev. Lett.* **1996**, *77*, 3865.
(29) *CRC Handbook of Chemistry and Physics*, 83rd ed.; Lide, D. R., Ed.; CRC Press: New York, 2002.
(30) Wycoff, R. W. G. *The Structure of Crystals*; The Chemical Catalog Company Inc.: New York, 1931.
(31) Villars, P. *Pearson's Handbook: Crystallographic Data for Intermetallic Phases*, desk ed.; ASM International: Materials Park, OH, 1997.
(32) The Inorganic Crystal Structure Database (ICSD). http://www.fiz-informationsdienste.de/en/DB/icsd/.
(33) Løvvik, O. M. *Phys. Rev. B* **2005**, *71*, 144111.
(34) Guette, A.; Barret, M.; Naslain, R.; Hagenmuller, P.; Tergenius, R.-E.; Lundstroem, T. *J. Less-Common Met.* **1981**, *82*, 325.

(35) Soulié, J.-P.; Renaudin, G.; Icrný, R.; Yvon, K. *J. Alloys Compd.* **2002**, *346*, 200.
(36) Wolverton, C.; Ozolinš, V.; Asta, M. *Phys. Rev. B* **2004**, *69*, 144109.
(37) Pinkerton, F. E.; Meisner, G. P.; Meyer, M. S.; Balogh, M. P.; Kundrat, M. D. *J. Phys. Chem. B* **2005**, *109*, 6.
(38) Aoki, M.; Miwa, K.; Noritake, T.; Kitahara, G.; Nakamori, Y.; Orimo, S.; Towata, S. *Appl. Phys. A* **2005**, *80*, 1409.
(39) Luo, W. *J. Alloys Compd.* **2004**, *381*, 284.
(40) Luo, W.; Sickafoose, S. *J. Alloys Compd.* **2006**, *407*, 274.
(41) Nakamori, Y.; Kithara, G.; Ninomiya, A.; Aoki, M.; Noritake, T.; Towata, S.; Orimo, S. *Mater. Trans.* **2005**, *46*, 2093.
(42) Leng, H.; Ichikawa, T.; Hino, S.; Hanada, N.; Isobe, S.; Fujii, H. *J. Phys. Chem. B* **2004**, *108*, 8763.
(43) Ichikawa, T.; Hanada, N.; Isobe, S.; Leng, H.; Fujii, H. *Mater. Trans.* **2005**, *46*, 1.
(44) Mal'tseva, N. N.; Golovanova, A. I.; Dymova, T. N.; Aleksandrov, D. P. *Russ. J. Inorg. Chem.* **2001**, *46*, 1793.
(45) Ozolinš, V.; Sadigh, B.; Asta, M. *J. Phys. Cond. Matt.* **2005**, *17*, 2197.
(46) Sun, Q.; Reuter, K.; Scheffler, M. *Phys. Rev. B.* **2003**, *67*, 205424.
(47) Himmel, H.-J. *Eur. J. Inorg. Chem.* **2003**, *2003*, 2153.
(48) Frankcombe, T. J.; Kroes, G.-J.; Züttel, A. *Chem. Phys. Lett.* **2005**, *405*, 73.
(49) Miwa, K.; Ohba, N.; Towata, S.; Nakamori, Y.; Orimo, S. *Phys. Rev. B* **2004**, *69*, 245120.